

Finite-State Markov Modeling for High-Speed Railway Fading Channels

Siyu Lin, *Member, IEEE*, Linghe Kong, *Member, IEEE*, Liang He, *Member, IEEE*,
Ke Guan, Bo Ai, *Senior Member, IEEE*, Zhangdui Zhong, and Cesar Briso-Rodríguez

Abstract—Developing an accurate and mathematically tractable high-speed railway (HSR) channel model is a key issue to provide reliable, cost-effective wireless services for the HSR operators and users. Although finite-state Markov chain (FSMC) has been extensively investigated to describe fading channels, most of FSMC channel models are designed based on the first-order Markov chain, which are no longer valid when the transceivers operate in high mobility scenarios, specially in HSR communications. In this letter, an advanced FSMC channel model for HSR is proposed, which incorporates the impacts of moving speed on the temporal channel statistical characteristic. The closed-form expressions of state transition probabilities between channel states are derived. The accuracy of the proposed FSMC channel model is validated via extensive measurements conducted on the *Zhengzhou-Xi'an* HSR line in China.

Index Terms—Fast time-varying fading channels, finite-state Markov chain, high-speed railway communications.

I. INTRODUCTION

HIGH-SPEED RAILWAYS (HSRs) have been widely deployed over the world because of their high capability in passenger transportation and low gas emission. Being a key subsystem of HSRs, the mobile communication system is required to provide reliable information transmission services for railway-specific signaling and efficient wireless multimedia services for passengers. As a result, an accurate description on the fading and the temporal variations of high-speed railway channels is highly demanded [1].

Although several physical layer channel models for HSRs exist in the literature [2]–[4], they are over-complex for upper-layer protocol design and performance analysis. On the other hand, *finite-state Markov chain* (FSMC) channel models can

provide accurate and mathematically tractable description of steady and temporal characteristic of fading channels [5], which have been extensively studied in different scenarios [6]–[11]. However, most existing FSMC channel models adopt the first-order Markov chain to describe their fading processes, such as [10], which are based on the simplified assumption that each channel state only transits to the adjacent states. This assumption may not be hold anymore in high-speed mobile systems such as HSRs due to the fast time-varying channel characteristic, e.g., the normalized fading rates of HSR channels $f_d\tau \geq 0.1$ [5], [12], where f_d is the Doppler shift and τ is the time slot duration. The impacts of moving speed on the temporal characteristic of fading channels are insufficiently tackled in the literature, which motivates us to reinvestigate the FSMC channel modeling for HSRs.

In this letter, we propose an advanced FSMC channel model for HSRs, which assists the performance evaluations and network design of HSR communications. The impacts of moving speed on the temporal channel statistical characteristic are incorporated in the proposed channel model. The channel states are defined based on their signal to noise ratios (SNRs) via the equal step-size partitioning method. Furthermore, a novel method in identifying the state transition probabilities of the fast time-varying channels is proposed to ensure the modeling accuracy. We validate the accuracy of the proposed model based on extensive measurements conducted on the *Zhengzhou-Xi'an* HSR line in China.

II. THE FINITE-STATE MARKOV CHAIN MODEL

To capture the variation of HSR fading channels, the channel states are defined according to their received SNR levels. We use FSMC to track their time-varying processes.

A. The Finite-State Markov Chain Model

Since the small-scale fading characteristic impacted by the moving speed is still a vacancy, in this letter, we mainly focus on the variation of small-scale fading in HSR channels.

In our modeling, we discretize the time into equal slots each of duration τ . Let γ_k denote the received SNR in the k th slot, where $\gamma_k \in [0, \infty)$. The range of SNR is divided into N nonoverlapping intervals with thresholds Γ_n ($n = 0, 1, 2, \dots, N$), where $\Gamma_0 = 0$ and $\Gamma_N = \infty$. The channel state is S_n ($n \geq 1$) when the received SNR falls in the SNR interval $[\Gamma_{n-1}, \Gamma_n)$. The slot duration τ and the SNR intervals should be selected carefully to keep the stability of channel state in one slot duration. Generally, the slot duration should be less than the coherent time and the range of SNR intervals should achieve well balance between accuracy and

Manuscript received October 30, 2014; revised December 12, 2014; accepted January 02, 2015. Date of publication January 07, 2015; date of current version April 21, 2015. This work was supported in part by the Fundamental Research Funds for the Central Universities (2013JBM147), by the National Science Foundation for Postdoctoral Scientists of China (2013M540846 and 2014M560334), by the National Natural Science Foundation of China (U1334202 and 61303202), by the State Key Laboratory of Rail Traffic Control and Safety (RCS2015K011), and by the Key Grant Project of Chinese Ministry of Education (313006). *Corresponding Author: Linghe Kong.*

S. Lin is with the School of Electronic and Information Engineering, Beijing Jiaotong University, Beijing, P.R. China (e-mail: sylin@bjtu.edu.cn).

L. Kong is with the Shanghai Jiao Tong University, Shanghai, P. R. China (e-mail: linghe.kong@sjtu.edu.cn).

L. He. is with the University of Michigan, Ann Arbor, USA.

K. Guan, B. Ai, and Z. Zhong are with the State Key Lab. of Rail Traffic Control and Safety, Beijing Jiaotong University, Beijing, P. R. China.

C. Briso-Rodríguez is with the Universidad Politécnica de Madrid, Spain.

Color versions of one or more of the figures in this letter are available online at <http://ieeexplore.ieee.org>.

Digital Object Identifier 10.1109/LAWP.2015.2388701

complexity. The details of slot duration and state number selection will be explained in Section IV-A.

It is clear that the channel state partition is the key factor that determines the accuracy and practicality of the FSMC channel model [5]. Different channel state partition methods exist in the literature, such as equal-probability method [13], equal-duration method [6], and equal step-size method [9]. In many modern mobile communication systems, such as LTE system, the effective SNR range is divided into several equal-size intervals in decibel. Each SNR interval corresponds to a channel quality indicator (CQI) value [14], which can be used for adaptive transmission schemes selection. So we select the equal step-size method to partition the SNR states as it is more practical for performance evaluation of mobile communication systems. The SNR interval size $\Delta\Gamma$ is calculated as, $\Delta\Gamma = \Gamma_n - \Gamma_{n-1} = \frac{\Gamma_{N-1} - \Gamma_1}{N-2}$, where Γ_{N-1} and Γ_1 are the thresholds of effective SNR range. For example, $\Gamma_1 = -9$ dB and $\Gamma_{N-1} = 20$ dB are adopted in LTE system [14].

B. FSMC Channel Model Parameters

In general, there is a dominant line of sight path in HSR channels making the Rician fading channel and Nakagami-m fading channel applicable [3], [11]. As Nakagami-m fading channel model is more mathematically tractable and Rician fading channel can be approximated by the Nakagami-m fading channel [15], the small-scale fading is modeled as Nakagami-m distribution in this work. Given the local mean SNR as Ω , the probability distribution function (PDF) of the received SNR of a Nakagami-m channel can be expressed as

$$f_\gamma(\gamma) = \left(\frac{m}{\Omega}\right)^m \frac{\gamma^{m-1}}{\Gamma(m)} \exp\left(-\frac{m\gamma}{\Omega}\right)$$

where $\Gamma(\cdot)$ is the Gamma function and m is the fading parameter. Next, we derive the key model parameters including the steady state probabilities and state transition probabilities.

Steady State Probability: With the Nakagami-m model, the steady state probability of state S_n can be calculated as

$$\pi_n = \int_{\Gamma_n}^{\Gamma_{n+1}} f_\gamma(\gamma) d\gamma = F_\gamma(\Gamma_{n+1}) - F_\gamma(\Gamma_n) \quad (1)$$

where $F_\gamma(\cdot)$ is the cumulative distribution function (CDF) of γ , specifically, $F_\gamma(\Gamma_n) = \frac{G(m, \frac{\Gamma_n m}{\Omega})}{\Gamma(m)}$, $G(s, x) = \int_0^x t^{s-1} \exp(-t) dt$.

State Transition Probability: To determine the state transition probabilities, an approximation method was proposed in [13], with which the transition probability from state S_n to state S_{n-1} is approximated to be the ratio of the level crossing rate at point Γ_{n-1} to the average number of symbols per second that is transmitted in the state S_n . The above approximation method is based on the assumption that the channel state only can transit to neighboring states in adjacent slots. However, the time-varying fading process of HSR cannot always be accurately captured by the first-order FSMC, especially for trains moving in high-speed. Therefore, we adopt the definition to determine the state transition probabilities. The state transition probability $p_{n,j}$ is defined as the probability that the channel state changes from S_n in the k th slot to S_j in the $(k+1)$ th slot. In other words, it is the probability that the fading channel amplitude moves from the n th SNR interval $[\Gamma_{n-1}, \Gamma_n)$ at the

k th slot to the j th SNR interval $[\Gamma_{j-1}, \Gamma_j)$ at the $(k+1)$ th slot, which can be calculated by integrating the joint PDF of the Nakagami-m fading channel over two consecutive time indices and over the desired intervals as

$$p_{n,j} = \frac{\int_{\sqrt{\Gamma_{n-1}}}^{\sqrt{\Gamma_n}} \int_{\sqrt{\Gamma_{j-1}}}^{\sqrt{\Gamma_j}} f_{R,2}(r_1, r_2; m, \rho) dr_1 dr_2}{\pi_n} \quad (2)$$

where r_1 and r_2 are the two samples of the Nakagami-m fading envelope at two adjacent slots, and $f_{R,2}(r_1, r_2; m, \rho)$ is the joint PDF of two correlated Nakagami-m random variables, which is given by [15]

$$f_{R,2}(r_1, r_2; m, \rho) = \frac{4m^{m+1}(r_1 r_2)^m}{\Gamma(m)\Omega_1\Omega_2(1-\rho)(\sqrt{\Omega_1\Omega_2\rho})^{m-1}} \cdot \exp\left(-\frac{m}{1-\rho}\left\{\frac{r_1^2}{\Omega_1} + \frac{r_2^2}{\Omega_2}\right\}\right) \cdot I_{m-1}\left(\frac{2m\sqrt{\rho}r_1 r_2}{\sqrt{\Omega_1\Omega_2}(1-\rho)}\right), \quad (3)$$

where $\Omega_i = E\{r_i^2\}$, $I_n(\cdot)$ is the n th order modified Bessel function of the first kind, ρ is the power correlation coefficient between the two samples, and $E\{\cdot\}$ represents the expectation operation. The correlation coefficient of two random variables R_1 and R_2 is defined as $\rho_{R_1, R_2} \triangleq \frac{\text{cov}\{R_1, R_2\}}{\sqrt{\sigma_{R_1}^2 \sigma_{R_2}^2}}$, where $\text{cov}\{\cdot\}$ denotes the covariance operation, and $\sigma_{R_1}^2, \sigma_{R_2}^2$ represent the variance of the random variables R_1 and R_2 , respectively. The most common correlation coefficient model of two SNR samples in adjacent slots can be expressed as [9]

$$\rho = J_0^2(2\pi f_d \tau) \quad (4)$$

where $J_0(\cdot)$ is the zero-order Bessel function of the first kind and f_d is determined by the moving speed. The correlation coefficient of two SNR samples also can be obtained according to the measurement results.

According to (2), the state transition probabilities between two channel states S_n and S_j can be expressed by the CDF of bivariate distribution as

$$p_{n,j} = (F_{R,2}(\sqrt{\Gamma_{n+1}}, \sqrt{\Gamma_{j+1}}; m, \rho) - F_{R,2}(\sqrt{\Gamma_n}, \sqrt{\Gamma_{j+1}}; m, \rho) - F_{R,2}(\sqrt{\Gamma_{n+1}}, \sqrt{\Gamma_j}; m, \rho) + F_{R,2}(\sqrt{\Gamma_n}, \sqrt{\Gamma_j}; m, \rho)) / \pi_n \quad (5)$$

where $F_{R,2}(u, v; m, \rho)$ is the corresponding CDF of bivariate distribution of two correlated Nakagami-m random variables

$$F_{R,2}(u, v; m, \rho) = \int_0^u \int_0^v f_{R,2}(r_1, r_2; m, \rho) dr_1 dr_2. \quad (6)$$

To calculate the CDF of bivariate Nakagami-m distribution, Lopez-Martinez *et al.* derived the exact closed-form expressions for positive integer fading factor m [16], which can be expressed as finite sum of elementary functions and bivariate confluent hypergeometric functions as (7), where $\Phi_3(b, c; w, z)$ is the confluent hypergeometric function, which (7), shown at the bottom of the next page, can be approximated by the sum of the first $(2l-1)$ terms

$$\Phi_3(b, c; w, z) \approx \sum_{k=0}^{2l-1} \frac{(b)_k \Gamma(c)}{k!} \frac{w^k}{z^{(c+k-1)/2}} I_{c+k-1}(2\sqrt{z})$$

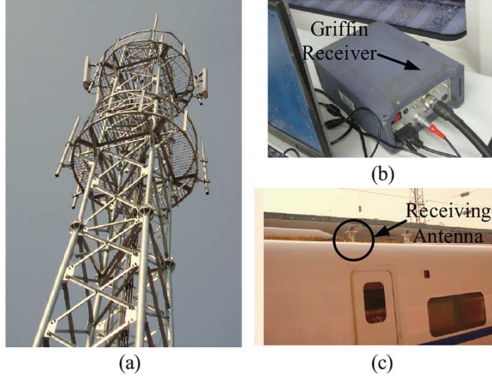


Fig. 1. Measurement scenario. (a) Transmitting antenna. (b) Willtek 8300 Griffin fast measurement receiver. (c) Receiving antenna.

and $(b)_k$ is the Pochhammer symbol defined as $(b)_0 = 1$ and $(b)_j = b(b+1)\cdots(b+j-1)$ ($j = 1, 2, \dots$).

III. MEASUREMENT CAMPAIGN

To evaluate the accuracy of the proposed FSMC model, we perform extensive measurements in the deployed *GSM-for-railway* (GSM-R) network of the *Zhengzhou-Xi'an* HSR line in China. In our measurements, existing base stations (BSs) of GSM-R network are adopted as the transmitters. The carrier frequency and bandwidth of BSs are 930 MHz and 200 KHz, respectively. The cross-polarization directional antennas (specifically, with 17-dBi gain, 43 dBm Tx power, 65° horizontal, 6.8° vertical beamwidths, and a height of 25–35 m above the rail surface) are connected to the BSs. The Willtek 8300 Griffin fast measurement receiver is adopted to collect the data. The omnidirectional receiver antenna is deployed on top of the high-speed trains, with 4-dBi gain, 80° vertical beamwidths, and a height of 30 cm above the train roof. The measurement scenario is shown in Fig. 1.

The measurement locations and train speed are collected via Global Positioning System (GPS) receiver and the distance sensor deployed on the wheel of the locomotive, respectively. To investigate the effects of moving speed on the temporal channel statistical characteristic, the trains move at two speed modes: low-speed mode (70–85 km/h) and high-speed mode (300–350 km/h). We sample SNRs at 3 cm intervals in low-speed mode and at 10 cm intervals in high-speed mode for small-scale fading.

IV. MODEL EVALUATION

The identified channel parameters of the proposed FSMC model are compared with measurement results.

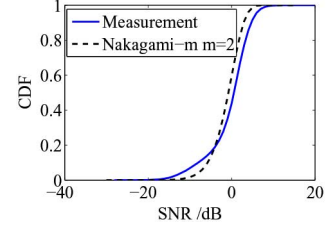


Fig. 2. CDF of the small-scale fading of measurement data and Nakagami- m channel model.

A. Parameters Selection

According to measurement setup, the carrier frequency of analysis model is 930 MHz. The highest movement speed of the train is 350 km/h, and the coherent time T_c of HSR channels can be approximated as $0.423/f_d \approx 1.4$ ms [17], which is also validated by measurement results [3]. The slot duration τ is selected as the transmission time slot of LTE system 1 ms [18], which is less than the coherent time T_c of HSR channels to ensure that the channel state is essentially invariant in one slot. The number of FSMC state is $N = 8$, which has been shown to well balance between accuracy and model complexity [5]. Although the HSR channels have much higher temporal variation on different SNR interval, the slot duration is less than the coherent time of HSR channels. So $N = 8$ is still applicable in HSR scenario.

The fading parameters and correlation coefficients in our model are selected according to the measurement results. The small-scale fading measurement results are collected by removing the effects of large-scale path loss from the raw measurement data. The 40-wavelength sliding window is used to average the raw measurement data for obtaining the large-scale path loss [3]. For HSR channels, the mean Rician K -factor is about 2.5 [3]. According to the relationship between Rician channel and Nakagami- m channel, $m = \frac{(K+1)^2}{2K+1}$, where K is Rician K -factor. Therefore, the fading parameter is set as $m = 2$. The CDFs of small-scale fading of measurement data and Nakagami- m channel model are shown in Fig. 2. It is found that the accuracy of fading parameter $m = 2$ can be accepted. Then we select $\Gamma_1 = -14$ dB and $\Gamma_{N-1} = 10$ dB according to the CDF of small-scale fading measurement data. Eq. (4) is selected as the correlation coefficient model, which can be transformed to $\rho = J_0^2(2\pi\Delta d f/c)$, where Δd indicates the sampling distance, f is the carrier frequency, and c is the speed of light. Fig. 3 shows the absolute values of envelope autocovariance of measurements and the correlation coefficients of the model. It can be seen that the correlation coefficient of the model can accurately describe the envelope autocovariance characteristic of HSR fading channels.

$$\begin{aligned}
 F_{R,2}(r_1, r_2; m, \rho) = & 1 - \sum_{k=0}^{m-1} \left[\exp\left(-\frac{mr_2^2}{\Omega_2}\right) \left(\frac{mr_2^2}{\Omega_2}\right)^k \frac{1}{k!} + \left(\frac{mr_1^2}{\Omega_1}\right)^k \frac{1}{k!} (1-\rho)^{-k} \exp\left(-\frac{m}{1-\rho} \left(\frac{r_1^2}{\Omega_1} + \frac{r_2^2}{\Omega_2}\right)\right) \right. \\
 & \cdot \left\{ \left(\frac{mr_2^2}{\Omega_2}\right)^k \frac{1}{k!} \Phi_3\left(1, k+1; \frac{r_2^2}{\Omega_2} \frac{m}{1-\rho}, \rho \left(\frac{r_1}{\sqrt{\Omega_1}} \frac{r_2}{\sqrt{\Omega_2}} \frac{m}{1-\rho}\right)^2\right) \right. \\
 & \left. \left. - \sum_{i=1}^{m-k} \left(\frac{mr_2^2}{\Omega_2}\right)^{k+i-1} \frac{1}{(k+i-1)!} \Phi_3\left(i, k+i; \frac{r_2^2}{\Omega_2} \frac{m\rho}{1-\rho}, \rho \left(\frac{r_1}{\sqrt{\Omega_1}} \frac{r_2}{\sqrt{\Omega_2}} \frac{m}{1-\rho}\right)^2\right) \right\} \right] \quad (7)
 \end{aligned}$$

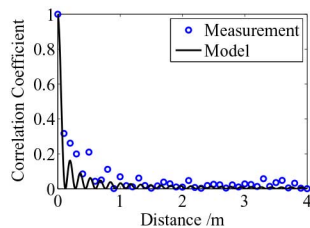


Fig. 3. Correlation coefficients of the envelope autocovariance function and measurement data.

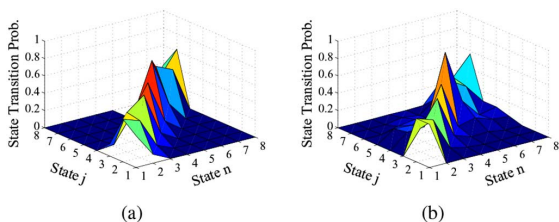


Fig. 4. State transition probabilities of the proposed model and measurement data under low-speed mode. (a) Analysis results. (b) Measurement results.

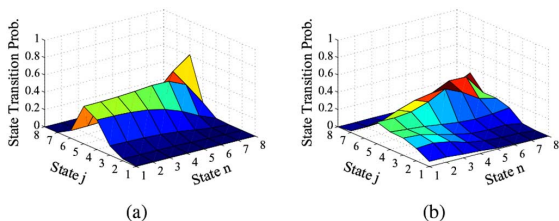


Fig. 5. State transition probabilities of the proposed model and measurement data under high-speed mode. (a) Analysis results. (b) Measurement results.

TABLE I
STEADY STATE PROBABILITIES

	$n=1$	$n=2$	$n=3$	$n=4$
Model	0.003	0.015	0.073	0.269
Measurements	0.017	0.044	0.066	0.221
	$n=5$	$n=6$	$n=7$	$n=8$
Model	0.465	0.172	0.003	4.33×10^{-8}
Measurements	0.397	0.195	0.058	0.003

B. Model Validation

The steady state probabilities of the proposed model and measurement data are compared in Table I. The state transition probabilities of the proposed model and measurement data at different speed modes are illustrated in Figs. 4 and 5. The comparisons show high similarity of the proposed FSMC model and the measurement data, which validate that the proposed model can accurately describe the steady and temporal channel statistical characteristic of HSR channels. The reason of the small gap between proposed model and measurements is that, the fading parameter of real HSR channel is not a constant, which varies at different locations.

Comparing the state transition probabilities under different speed modes shown in Figs. 4 and 5, we find that, the channel states only transit to neighboring channel states at the low speed mode but the channel states transit to further states at the high speed mode. This is because that, the normalized fading rates change from $f_d\tau \approx 0.075$ in low speed mode to $f_d\tau \approx 0.25$, which leads the correlation between the two samples in adjacent slots becoming weak. It means that the fading process should be

described by high-order Markov chain in the high speed mode. Furthermore, Figs. 4 and 5 show that our proposed model can break the assumption of first-order Markov chain to accurately describe the temporal channel statistical characteristic at any speed conditions.

V. CONCLUSION AND FUTURE WORK

In this letter, an advanced FSMC channel model was proposed for HSR fading channels. We derived the generalized closed-form expression of state transition probabilities, which is free for any moving speed. We referred the LTE system to set the channel parameters, so the proposed model is practical, and its accuracy was validated by extensive measurements. We concluded that the fast time-varying fading channel should be modeled by the high order or even memoryless Markov model to guarantee the model accuracy.

REFERENCES

- [1] B. Ai, X. Cheng, T. Kurner, Z.-D. Zhong, K. Guan, R.-S. He, L. Xiong, D. Matolak, D. Michelson, and C. Briso-Rodriguez, "Challenges toward wireless communications for high-speed railway," *IEEE Trans. Intell. Transp. Syst.*, vol. 15, no. 5, pp. 2143–2158, Oct. 2014.
- [2] H. Wang, F. Yu, L. Zhu, T. Tang, and B. Ning, "Modeling of communication-based train control (CBTC) radio channel with leaky waveguide," *IEEE Antennas Wireless Propag. Lett.*, vol. 12, pp. 1061–1064, 2013.
- [3] R. He, Z. Zhong, B. Ai, G. Wang, J. Ding, and A. F. Molisch, "Measurements and analysis of propagation channels in high-speed railway viaducts," *IEEE Trans. Wireless Commun.*, vol. 12, no. 2, pp. 794–805, Dec. 2013.
- [4] K. Guan, Z. Zhong, B. Ai, and T. Kurner, "Propagation measurements and modeling of crossing bridges on high-speed railway at 930 MHz," *IEEE Trans. Veh. Technol.*, vol. 63, no. 2, pp. 502–517, Feb. 2014.
- [5] P. Sadeghi, R. A. Kennedy, P. B. Rapajic, and R. Shams, "Finite-state markov modeling of fading channels—a survey of principles and applications," *IEEE Signal Process. Mag.*, vol. 25, no. 5, pp. 57–80, Nov. 2008.
- [6] Q. Zhang and S. A. Kassam, "Finite-state markov model for rayleigh fading channels," *IEEE Trans. Commun.*, vol. 47, no. 11, pp. 1688–1692, Nov. 1999.
- [7] C. Pimentel, T. H. Falk, and L. Lisbôa, "Finite-state markov modeling of correlated rician-fading channels," *IEEE Trans. Veh. Technol.*, vol. 53, no. 5, pp. 1491–1501, Sep. 2004.
- [8] R. Zhang and L. Cai, "A packet-level model for uwb channel with people shadowing process based on angular spectrum analysis," *IEEE Trans. Wireless Commun.*, vol. 8, no. 8, pp. 4048–4055, Aug. 2009.
- [9] M. A. Juang and M. B. Pursley, "New results on finite-state markov models for nakagami fading channels," in *Proc. MILCOM'11*, 2011, pp. 453–458.
- [10] S. Lin, Z. Zhong, L. Cai, and Y. Luo, "Finite state markov modeling for high speed railway wireless communication channel," in *Proc. GLOBECOM'12*, 2012, pp. 5421–5426.
- [11] H. Wang, F. R. Yu, L. Zhu, T. Tang, and B. Ning, "Finite-state markov modeling for wireless channel in tunnel communication-based train control (CBTC) systems," *IEEE Trans. Intell. Transp. Syst.*, vol. 15, no. 3, pp. 1083–1090, Jun. 2014.
- [12] F. Babich, O. E. Kelly, and G. Lombardi, "Generalized markov modeling for flat fading," *IEEE Trans. Commun.*, vol. 48, no. 4, pp. 547–551, Apr. 2000.
- [13] H. S. Wang and N. Moayeri, "Finite-state markov channel—a useful model for radio communication channels," *IEEE Trans. Veh. Technol.*, vol. 44, no. 1, pp. 163–171, Feb. 1995.
- [14] J. C. Ikuno, M. Wrulich, and M. Rupp, "System level simulation of LTE networks," in *Proc. VTC'10-Spring*, 2010, pp. 1–5.
- [15] M. Nakagami, "The m-distribution—a general formula of intensity distribution of rapid fading," *Statist. Method Radio Propag.*, 1960.
- [16] F. Lopez-Martinez, D. Morales-Jimenez, E. Martos-Naya, and J. Paris, "On the bivariate nakagami-m cumulative distribution function: Closed-form expression and applications," *IEEE Trans. Commun.*, vol. 61, no. 4, pp. 1404–1414, Apr. 2013.
- [17] T. S. Rappaport, *Wireless Communications Principles and Practice*. Englewood Cliffs, NJ, USA: Prentice Hall, 2002.
- [18] 3GPP, "Physical layer aspect for evolved universal terrestrial radio access (UTRA)," Oct. 2006 [Online]. Available: <http://www.3gpp.org/DynaReport/25814.htm>, 3GPP, TS 25.814